Tidal effects on runup in presence of complex 3D morphologies under dissipative surf zone conditions

Nadia Senechal[1] , Giovanni Coco[2], Karin Bryan[3], Jamie MacMahan[4], Jenna Brown[4] and Rob Holman[5]

Abstract

Runup dynamics were investigated on a sandy barred beach using data obtained from video images under stationary energetic conditions. Runup was estimated at both high and low tides at four cross-shore positions. Significant runup height was found to vary by a factor of 1.3 between low and high tide and was found to be dominated by infragravity energy, consistent with the dissipative conditions. The drop in infragravity energy observed in the runup variance at low tide is associated with a drop in infragravity energy in the inner surf zone on the inner sandbar. Data also show that while beach slope and offshore wave characteristics are significantly correlated to runup elevation at high tide, as predicted by existing theories, no significant correlation is observed at low tide suggesting that the water level above the bar plays a critical role.

Key words: video, inner bar, infragravity energy, runup, swash zone

1. Introduction

Wave-induced runup is one of the critical parameters when estimating the probability and effects of coastal inundation and when studying the physical processes contributing to beach erosion/accretion (e.g., Masselink and Hughes, 1998; Puleo et al., 2000**;** Elfrink and Baldock, 2002). Predicting wave runup elevations for a given offshore climate is extremely complicated and even the most recently developed formulations do not explain the variability encountered in the field (e.g., Stockdon et al., 2006; Senechal et al., 2011; Guedes et al., 2011).

At present, wave runup is estimated using empirical formulas that relate beach slope and offshore wave characteristics to runup elevations. A generally-accepted nondimensional parameter linking information related to beach and wave characteristics is the Iribarren number, which is defined as:

$$\xi_0 = \frac{\tan\beta}{\left(H_0 / L_0\right)^{1/2}} \tag{1}$$

where β is the beach slope, L_0 is the deep water wave length given by linear theory and H_0 is the offshore wave height. Dissipative conditions are generally associated with low values of Iribarren parameters, typically less than 0.3 (Stockdon et al., 2006; Ruggiero et al., 2001; Ruessink et al., 1998, Raubenheimer and Guza, 1996; Raubenheimer et al., 1995; Guza and Thornton, 1982), whereas intermediate and reflective conditions are associated to larger values (Holland and Holman, 1999; Holland, 1995; Holman, 1986; Holman and Sallenger, 1985).

However, recent works have already indicated that large- (Ruggiero et al., 2004) and small-scale (Bryan and Coco, 2010) alongshore variations in beach slope give rise to a range of behaviours that complicates prediction of runup height. Guedes et al. (2011) also showed that under mild offshore wave conditions, the presence of a sandbar and the tidally controlled water-depth over its crest generated important variations

[1]UMR EPOC, University of Bordeaux, Avenue des Facultés, Talence 33405, France. N.senechal@epoc.u-bordeaux1.fr
[2]Environmental Hydraulics Institute, "IH Cantabria", Universidad de Cantabria, Santander, Spain
[3]Dept. of Earth and Ocean Sciences, University of Waikato, Hamilton, New Zealand
[4]Naval Postgraduate School, Monterey, U.S.A
[5] CEOAS, Oregon State University, Corvallis, USA.

(by a factor 2) of significant runup height because of the differences in wave transformation.
The objective of this work is to further investigate tidal effects on swash motions and runup height under dissipative surf zone conditions and in presence of large-scale (order of a hundred meters) morphological features. Notice that we here use the term "large-scale" not in absolute sense but relative to previous runup studies that have primarily focused on the analysis of individual transects or transects that are closely spaced (order of meters).

2. Material and Methods

2.1. *Field area*

Data presented in this work were obtained during the ECORS-Truc Vert'08 Beach experiment (Senechal et al., 2011b). The field site (Figure 1) is situated on the southern part of the French Atlantic coast and is typical of the relatively natural coast extending between the Gironde Estuary (90 km to the north) and the Arcachon inlet (10 km to the south). The sediment consists primarily of medium grained quartz sand whose mean surface grain size varies with the morphology, with coarser sediments (~0.6 mm) observed in the deeper rip channels and finer sediments (~0.3 mm) observed on the shoals between the rips (Gallagher et al., 2011). Truc Vert beach exhibits complex three-dimensional and highly dynamic morphologies commonly involving two distinct sandbar systems. The inner bar (see Figure 1) can experience all the states within the intermediate classification (see Wright and Short, 1984; Masselink and Short, 1993). The outer bar system exhibits persistent crescentic patterns at a narrow range of wavelengths with a shape varying from symmetric to asymmetric (Castelle et al., 2007). The field site experiences an annual mean spring tidal range of 3.7 m. Alongshore tide-driven currents in the nearshore zone are negligible. The wave climate is energetic with an annual mean significant wave height of 1.36 m and mean period around 8 s associated with long distance swells travelling mainly from N-NW directions (Butel et al., 2002).

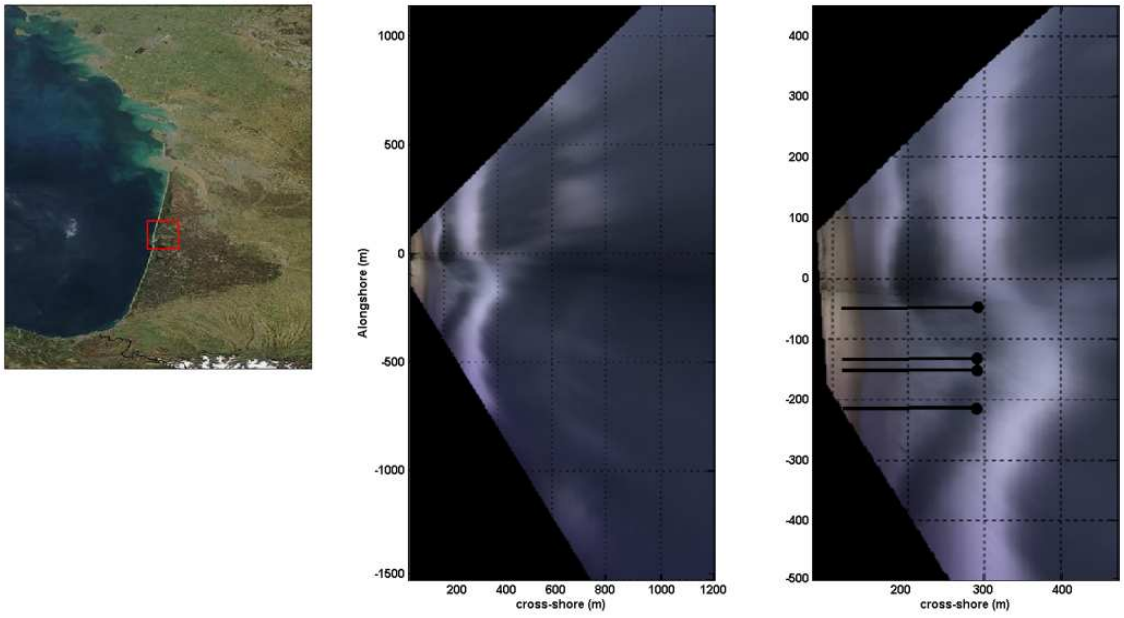

Figure 1. Field site Truc Vert Beach situated on the southwest part of the French Atlantic Coast.. (Middle)10-min Rectified and merged images at low tide on March, 14th. Limited breaking is observed over the offshore sandbar (located approximately at cross-shore position 700m). (Right) Zoom of the inner bar system and positions of the transects and PUV sensors (black circles).

2.2. *Data*

Sea state conditions were measured with a directional Mark III Datawell waverider buoy anchored in 20 m depth situated offshore of the field area, about 1.5 kms from the beachface. A synchronous, 5Hz coherent 7-element alongshore-lagged array of co-located pressure and horizontal digital electromagnetic velocity sensors (hereafter PUV) mounted to pipes jetted along the inner bar was used to evaluate the wave characteristics in the surf zone (Figure 1, Right). The instruments were located approximately 35cm from the seabed, cabled to the shore and time-synced to an onshore GPS clock. Throughout the experiment, runup was measured with a video system mounted on an 8-m high scaffolding built on the top of the dune backing the beach and time-synced to a GPS clock. The height of the two high-resolution digital cameras was about 27 m above mean sea level. Overlap in the field of view of the two cameras allowed for continuous coverage of , an alongshore distance of about 600 m at high spring tide. As our main interest was in tidal effect on runup in presence of complex 3D morphologies, the data discussed in this paper will focus on two periods: one centered around low tide and the other centered around high tide. Data were collected under neap tide conditions to allow for the collection of longer (stationary) data series and for the estimation of runup onshore the PUV sensors deployed along the inner bar,. The data discussed below consist of 116 15-min wave runup elevation time series measured along 4 individual cross-shore transects (Figures 1&2) centered on both low and high tides. The sampling frequency of the video system and of the derived runup time series was 2 Hz. Positions of the transects were onshore the PUV sensors deployed along the inner bar system. The mean water level elevations for the time series considered, according to in-situ pressure measurements, varied by less than 0.4 m for each selected period (high and low tide). Variation in mean water depth between high and low tide periods reached 1.6m.

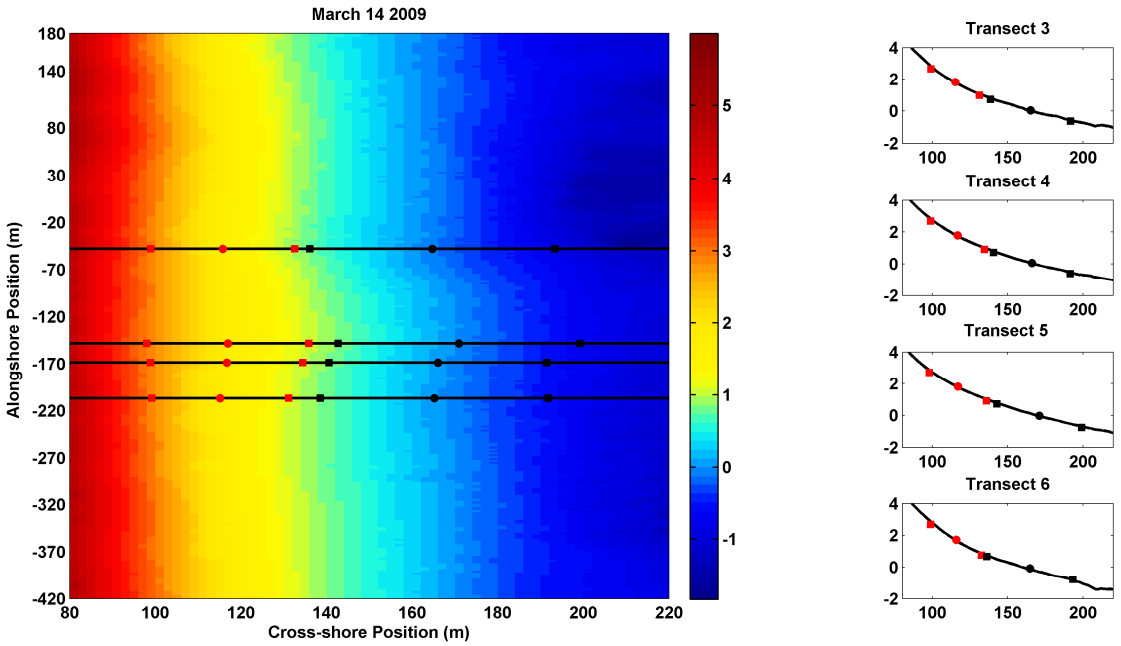

Figure 2. (Left) Intertidal topographic surveys with transects where runup were estimated. Red and black symbols respectively represent high and low mean shoreline positions and swash zone limits (defined as the mean ± 2 standard deviation). (Right) Cross-shore profile from transects.

2.3. *Data processing*

Runup (Figure 2) was manually digitized by two operators. The same methodology as presented in

Sénéchal et al. (2011a) was applied. Runup and rundown were identified as a white edge moving back and forth in the swash zone. To extract runup elevations along individual transects from video, the topography of the beach is needed in addition to the geometry of the cameras. To obtain the beach surface topography, a survey using Real Time Kinematic Differential Global Positioning System (RTK DGPS) was performed at each low tide (see Parisot et al., 2009). Photogrammetric relationships were used to convert the digitized runup into time series of water level elevation relative to the French National datum. The vertical resolution of the runup elevation, depending both on lens properties and distance from the cameras, was estimated by mapping the horizontal pixel resolution (typically < 1.0 m) to the elevation along the cross-shore transect. The vertical resolution was less than 0.08 m for all the data analyzed. Energy spectra, PSD (f), were computed from detrended, tapered data segments of 1800 points (900 s). The runup and surf zone data were then partitioned to determine the incident band component (0.05 Hz < f < 0.24 Hz) and the infragravity band component (0.004 Hz < f < 0.05 Hz). Runup and surf zone heights, *S*, were calculated as:

$$S = 4 * \sqrt{\sum PSD(f)df} \tag{2}$$

Runup and surf zone heights in the incident band, S_{inc}, and in the infragravity band, S_{ig}, were calculated by summing only over frequencies within the specified limits. Finally, the definition of the foreshore beach slope β in this study was taken, in agreement with other studies of swash zone hydro- and morphodynamics (Coco et al., 2004; Ruggiero et al., 2004) to be the linear slope within the region between $\pm$ two standard deviations from the mean runup elevation.

3. Results

3.1. *Environmental Conditions*

The periods selected for analysis correspond to the remarkably stationary period experienced over the first tidal cycle of March, 14th (see Table 1 and rectangles in Figure 3). This period was also selected because neap tide conditions allowed covering nearly 4-hour consecutive periods at both high and low tides with weak variations in mean sea surface elevation (typically less than 0.4m), allowing thus limited variations in the effective swash topography and surf zone bathymetry. Conditions during this period were moderate in comparison to the storm experienced by the area 3 days before (H_0 up to 8 m). The mean offshore significant wave height was nearly 2 m and the incident wave period was also very long with a mean value of 13.3 s. It varied by a factor of 1.13 between low and high tide. Wave dissipation on the outer bar was relatively weak even at low tide (see Figure 1 Middle), certainly because the high-energy wave conditions experienced during the storm on March, 11th induced an up-state transition of the outer bar associated with an offshore migration of some 100 m (Almar et al., 2010). Thus waves were breaking essentially on the inner bar, as denoted by the foam spatial patterns observed on Figure 1.

Beach profiles exhibited concave profiles (Figure 2) and $\beta_{2\sigma}$ slopes (the linear slope within the region comprised within $\pm$ two standard deviations from the mean run-up elevation) were relatively gentle, typically less than 0.030 on the lower intertidal domain (at low tide) and steeper on the upper beachface (Table 1), typically greater than 0.045 (at high tide) consistent with the highly dissipative conditions experienced the days before. Alongshore range of foreshore beach slope was less than 0.007 at low tide and 0.016 at high tide accounting for an increase of 35% from the smallest to the highest value for each period. Alongshore variation in $\beta_{2\sigma}$ slopes was substantially lower than the ones previously reported in the literature focusing on alongshore variability in swash motions (e.g. Ruggiero et al., 2004; Guedes et al., 2012) and mean alongshore value of Iribarren numbers fills the gap between extremely dissipative conditions (e.g., Ruggiero et al., 2004) and more reflective conditions (e.g., Guedes et al., 2012).

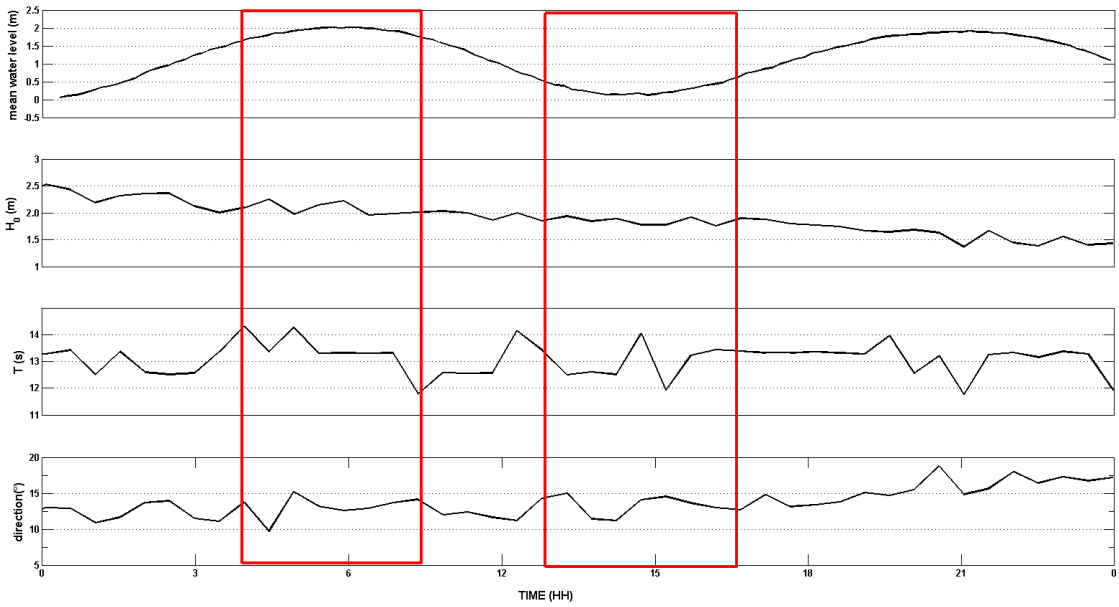

Figure 3. Environmental parameters. (Upper) mean water level as measured on the inner bar in the surf zone. (Middle) Offshore significant wave height (m). Peak period (s) and (Lower) Wave direction from Normal (°).

Table1. Environmental parameters: mean water level (m), offshore significant wave height (m), offshore period (m), offshore wave direction from normal to the beach (°), 'swash' slopes and Iribarren number.

	High Tide		**Low Tide**	
	Mean	**Std**	**Mean**	**Std**
Water Level (m)	1.89	0.11	0.29	0.14
H_0 (m)	2.10	0.12	1.85	0.07
T (s)	13.6	0.47	13.0	0.66
Θ (°) from Normal	12.5	1.7	12.5	1.4
$\beta_{2\sigma}$	0.053	0.005	0.026	0.002
Iribarren number ξ_0	0.487	0.052	0.235	0.021

3.2. *Runup dynamics*

Figure 4 shows the averaged spectra at high (red) and low (black) tide. Averaged spectra were calculated averaging spectra from all the 15-min time series for each transect respectively at High and Low tide, resulting in 28 degrees of freedom with a bandwidth of 0.0011 Hz. We observe that the spectra are tidally modulated both in energy levels but also in shape. For all transects, the average runup spectra reveal a saturated region that decayed approximately between f^{-4} and f^{-3}, consistent with previous observations (Guza and Thornton, 1982; Ruessink et al. 1998; Ruggiero et al., 2004; Guedes et al., 2011). The knickpoint between the saturated and unsaturated part was estimated using the method described by Ruessink et al. (1998) and ranged from 0.021 Hz to 0.033 Hz with a mean of 0.025 Hz for the runup spectra at low tide while at high tide the knickpoint was generally above 0.04Hz but less than 0.05Hz; that is, the saturated tail extended into the infragravity-frequency band consistent with previous observations (Ruessink et al., 1998; Ruggiero et al., 2004). The shift of the knickpoint towards lower frequencies at low tide, results in an overall decay of energy observed at the high frequencies of the infragravity band between high and low tide while lower frequencies were generally less affected. Consistent with spectra collected under energetic conditions (e.g., Ruessink et al., 1998) no significant peak (at confidence level 0.95) was observed in the infragravity band at high tide even though most of the energy variance is concentrated well below the 0.05 cut-off. At low tide three transects (3, 4 and 5) showed significant peaks.

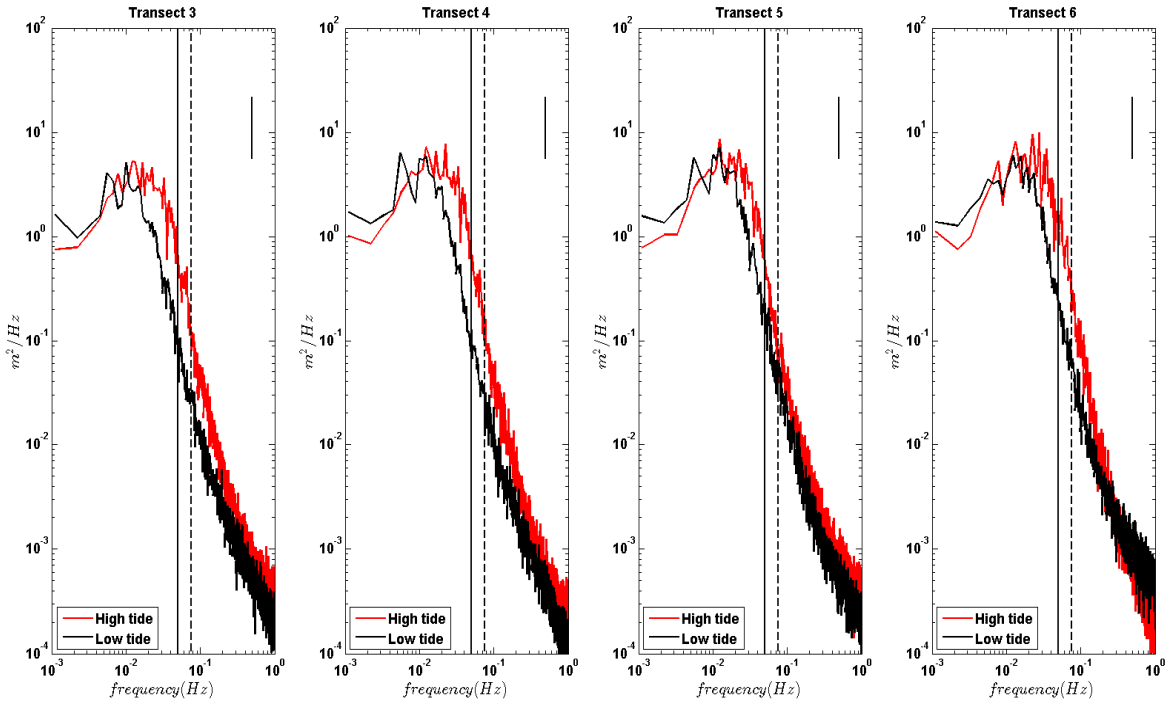

Figure 4. Averaged runup spectra at the four different transects. Solid vertical line indicates the limit between infragravity and incident bands. Dashed vertical line indicates offshore incident peak frequency.

A summary of run-up parameters, obtained from the individual spectra is given in Table 2. Table 2 shows that the mean significant vertical run-up elevation S during this period was 1.6 m at high tide and 1.2 m at low tide. It varied by a factor of 1.3 between low and high tide but was less variable for each period (high and low tide). The mean infragravity component (respectively 1.52 m and 1.17 m at high and low tide) was higher than the incident one (respectively 0.45 m and 0.23 m) by a factor up to 5. In contrast to the results presented by Guedes et al. (2011), the energy in the infragravity band of the runup is enhanced at high tide. Table 2 also shows that the vertical run-up was dominated by infragravity waves during most runs with the ratio S_{ig}/S having an average value of 0.96, similar to the previous values reported in the literature under highly dissipative conditions (Stockdon et al., 2006; Ruggiero et al., 2004; Ruessink et al., 1998).

Table 2. Summary of runup parameters.

	High Tide		**Low Tide**	
	Mean	**Std**	**Mean**	**Std**
S (m)	1.60	0.23	1.20	0.15
S_{ig} (m)	1.52	0.22	1.17	0.15
S_{in} (m)	0.45	0.12	0.23	0.04
S_{ig}/S	0.95	0.02	0.98	0.01
$\%S^2_{ig}$	92	3.4	96	1.26

As shown in Figure 5 and Table 3, the total vertical run-up elevation S is not significantly correlated to offshore wave parameters $(H_0 L_0)^{1/2}$, which was expected given the stationarity of offshore wave conditions over the tidal cycle. This is also consistent with Guedes et al. (2011). On the other side, we observe a dependence of S on $\beta_{2\sigma} (H_0 L_0)^{1/2}$ consistent with previous field studies (Holman and Sallenger, 1985; Ruggiero et al., 2004). The presence of a high intercept (arising because of the saturated incident conditions) is somewhat counter-intuitive as it implies a vertical run-up of 0.78 m without waves. Forcing the fit linear line to intercept at 0 drastically decreases the coefficient correlation to a not significant value.

We also observe that there is a different behavior between high (red symbols) and low tide (black symbols). Indeed, when we consider only the values obtained during low tide we observe that taking into consideration the beach slope $\beta_{2\sigma}$ does not improve the results and that linear regression are statistically not significant. This is opposite to what Guedes et al. (2011) observed in their data set. Indeed, by regression S against $\beta_{2\sigma}$, they noticed that the correlation coefficient r^2 jumped from ~0 to 0.52 when their high-tide runs were excluded from the analysis. However, their data were collected along one single transect whereas in the preset study, data were collected along four transects in presence of a complex beach topography (Figures 1 and 2).
Even if data presented here were collected under similar offshore conditions, the bathymetry over which the waves propagated presented complex 3D-patterns whose shape changed under varying water levels due to the tide. To evaluate possible alongshore variations in surf zone forcing, data collected in the surf zone on the inner bar were further investigated.

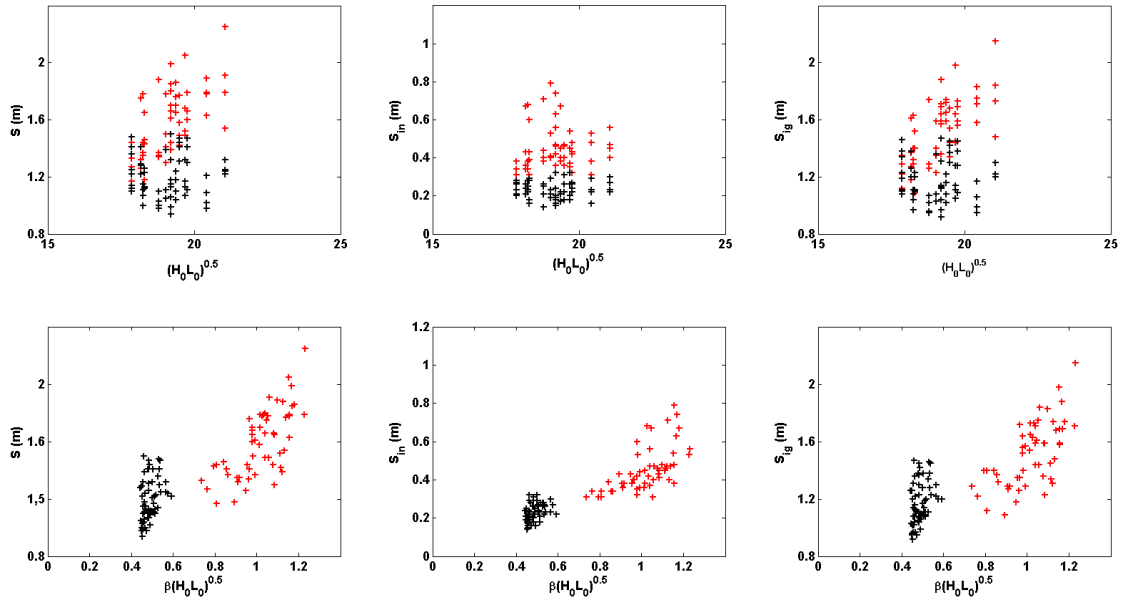

Figure 5. Total, S (left panels), infragravity, S_{in} (middle panels), and incident S_{ig} (right panels) runup elevation versus environmental parameters. Red symbols refer to high tide data and black symbols to low tide data.

3.3. *Surf zone dynamics*

Figure 6 shows the averaged spectra at high (red) and low (black) tide at PUV sensors on the inner bar. Averaged spectra were calculated similarly to the ones of the runup time series by averaging spectra estimated from all the 15-min time series for each PUV sensor respectively at High and Low tide, resulting in 28 degrees of freedom with a bandwidth of 0.0011 Hz. We clearly observe that the spectra are tidally modulated due to the degree of wave breaking over the inner sandbar. In particular we observe that in the incident band both the primary and the first harmonic (around 0.15 Hz) severely dropped between high and low tide conditions certainly due to enhanced wave breaking over the inner sandbar. On the other side, more surprising is the drop in infragravity energy observed between high and low tide (Table 4) by a factor of nearly 30%, even if at low tide energy levels observed in infragravity energy are still of the same order of magnitude as the one observed in the incident band.
Our observations do not fit the usual way because one would expect a higher level of infragravity energy at low tide when the wave energy dissipation of the inner sandbar is enhanced as reported in many other studies (e.g. Ruessink, 1998; Baldock and Huntley, 2001; Janssen et al., 2003; Guedes et al., 2011) showing that wave breaking is key to the increase of infragravity energy in the surf zone. However different hypothesis should be further investigated among them infragravity saturation (e.g. Battjes et al.,

2004; Van Dongeren et al., 2004, 2007; Hendersen et al., 2006; Thomson et al., 2006), the role of the inner sandbar on the infragravity energy (e.g. Bryan et al., 1998; Almar et al., 2012) and the role of alongshore currents (Bryan and Bowen., 1998).

Table 3. Y=mX+b. Correlation coefficient squared r^2 significant at the 99% confidence level showed in bold.

	Dependent variable	Independent variables	m	b	r^2
All data	S_t	$(H_0L_0)^{1/2}$	0.09	-0.31	0.08
		$\beta_{2\sigma}(H_0L_0)^{1/2}$	0.81	0.78	**0.67**
		$\beta_{2\sigma}(H_{sz}L_0)^{1/2}$	1.06	0.96	**0.63**
	S_{ig}	$(H_0L_0)^{1/2}$	0.09	-0.35	0.09
		$\beta_{2\sigma}(H_0L_0)^{1/2}$	0.73	0.81	**0.61**
		$\beta_{2\sigma}(H_{sz}L_0)^{1/2}$	0.94	0.96	**0.58**
	S_{in}	$(H_0L_0)^{1/2}$	0.11	0.01	0.01
		$\beta_{2\sigma}(H_0L_0)^{1/2}$	0.43	0.01	**0.74**
		$\beta_{2\sigma}(H_{sz}L_0)^{1/2}$	0.57	0.11	**0.70**
High Tide	S_t	$(H_0L_0)^{1/2}$	0.17	-1.61	**0.38**
		$\beta_{2\sigma}(H_0L_0)^{1/2}$	1.37	0.21	**0.48**
		$\beta_{2\sigma}(H_{sz}L_0)^{1/2}$	2.2	0.25	**0.40**
	S_{ig}	$(H_0L_0)^{1/2}$	0.17	-1.76	**0.44**
		$\beta_{2\sigma}(H_0L_0)^{1/2}$	1.23	0.28	**0.42**
		$\beta_{2\sigma}(H_{sz}L_0)^{1/2}$	2.00	0.30	**0.37**
	S_{in}	$(H_0L_0)^{1/2}$	0.01	0.21	0.01
		$\beta_{2\sigma}(H_0L_0)^{1/2}$	0.61	-0.17	**0.38**
		$\beta_{2\sigma}(H_{sz}L_0)^{1/2}$	0.93	-0.12	**0.29**
Low Tide	S_t	$(H_0L_0)^{1/2}$	0.00	1.20	0.00
		$\beta_{2\sigma}(H_0L_0)^{1/2}$	1.54	0.46	**0.30**
		$\beta_{2\sigma}(H_{sz}L_0)^{1/2}$	2.68	0.20	0.13
	S_{ig}	$(H_0L_0)^{1/2}$	0.00	1.19	0.00
		$\beta_{2\sigma}(H_0L_0)^{1/2}$	1.52	0.43	**0.35**
		$\beta_{2\sigma}(H_{sz}L_0)^{1/2}$	2.66	0.19	0.13
	S_{in}	$(H_0L_0)^{1/2}$	0.00	0.23	0.00
		$\beta_{2\sigma}(H_0L_0)^{1/2}$	0.44	0.01	0.13
		$\beta_{2\sigma}(H_0L_0)^{1/2}$	0.52	0.04	0.07

To further investigate the role of tidally modulated offshore conditions on runup parameter Figure 7 illustrates runup parameters as a function of surf zone parameters. Values obtained from the linear regression are reported in table 3.While for high tide, using surf zone heights estimated on the inner bar does not statistically change the patterns, for low tide data, regression are significantly improved as the correlation coefficient r^2 jumps from ~0 to 0.35 for the infragravity component of the runup. This result indicates that the presence of the tidally modulated water level above the inner bar seems to be a key parameter in the control of infragravity energy in the runup.

Table 4. Summary of surf zone parameters

	High Tide		Low Tide	
	Mean	**Std**	**Mean**	**Std**
H (m)	0.76	0.04	0.38	0.03
H_{ig} (m)	0.35	0.05	0.27	0.02
H_{in} (m)	0.67	0.04	0.27	0.04
H_{ig}/H	0.46	0.05	0.70	0.06
$\%H^2_{ig}$	22	5	50	9

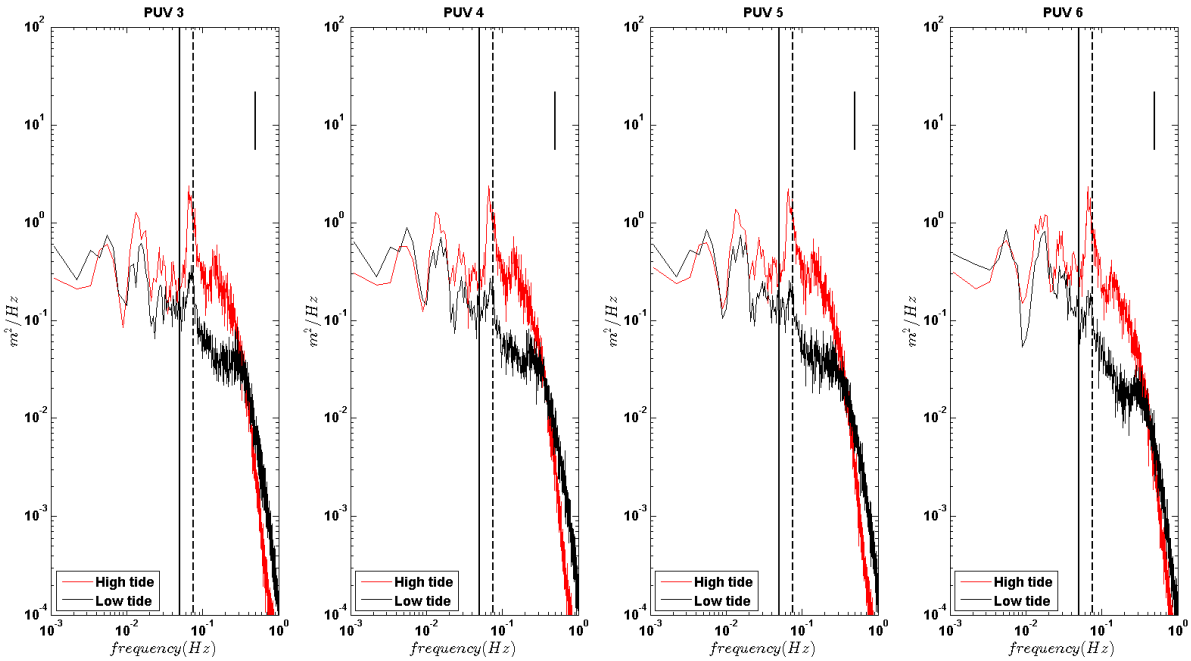

Figure 6. Averaged surf zone elevation spectra at the four different PUV sensors. Solid vertical line indicates the limit between infragravity and incident bands. Dashed vertical line indicates offshore incident peak frequency.

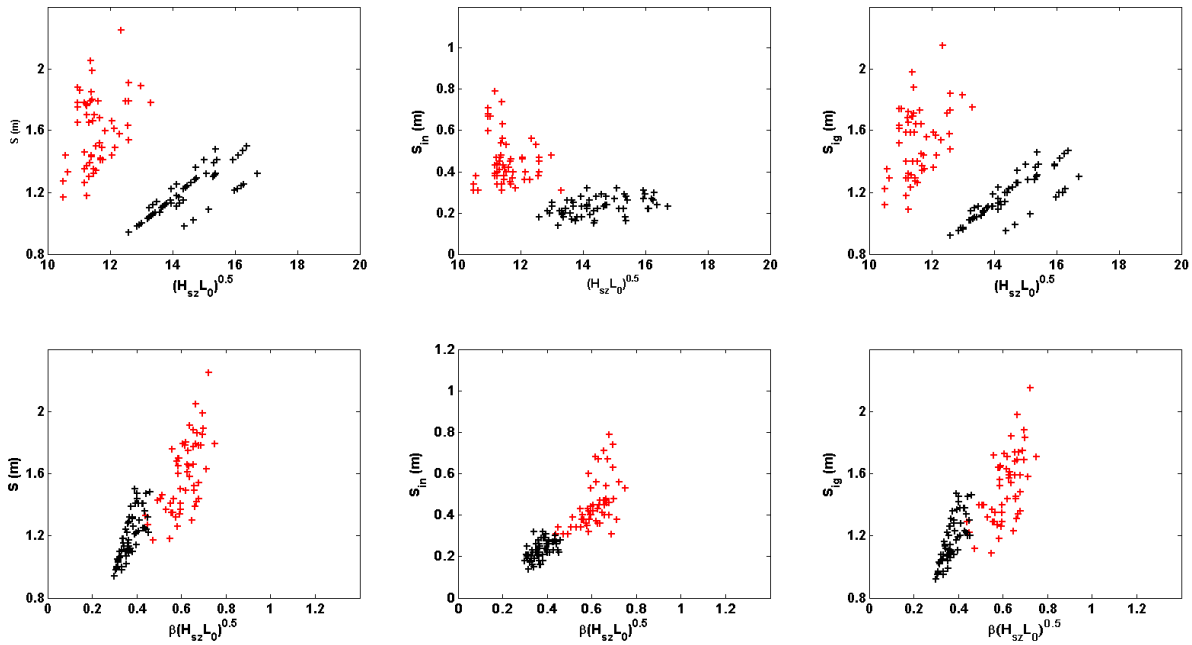

Figure 7. Total, S (left panels), infragravity, S_{in} (middle panels), and incident S_{ig} (right panels) runup elevation versus surfzone parameters (surfzone significant wave height instead of offshore significant wave height was used here). Red symbols refer to high tide data and black symbols to low tide data.

4. Conclusions

Runup time series collected along four transects in presence of a complex beach topography were observed to be strongly modulated by tide under energetic stationary wave conditions. Runup dynamic was found to be dominated by infragravity energy, consistent with the low Iribarren parameters. However, infragravity energy in the runup time series drastically dropped between high and low tide (nearly 30%). Analyses of data collected in the surf zone indicate that at the same time, infragravity energy in the inner surf zone also drastically dropped by nearly 30%. Data also suggest that runup elevations are not correlated to offshore environmental parameters. Accounting for the beach slope drastically increases the correlation at high tide but, no statistically correlation is observed at low tide. On the other hand, accounting for wave height in the surf zone on the inner bar, drastically increase the correlation at low tide. These preliminary results suggest that at high tide, the inner sandbar does not play a crucial role in runup dynamic that is essentially driven by offshore environmental forcing and local beach slopes. On the other hand, at low tide, the presence of the bar seems to play a crucial role in the drop of infragravity energy, resulting in a drop of runup elevation. Further analysis is under way to better access the critical role played by the 'large scale' morphology (here the inner sandbar) and the local parameters.

Acknowledgements

We wish to thank all the organizations that have provided financial support for the field experiment, in particular the French DGA (ECORS project). Thanks also to Rafael Almar, George Payne, Vincent Marieu and Antoine Réjas for the support in the installation of the video system, Jean-Paul Parisot, Sylvain Capo and Stephan Bujan for the RTK DGPS data. This work was conducted within the Research Program ANR-Jeunes Chercheurs BARBEC.

References

Almar, R., B. Castelle, B.G. Ruessink, N. Senechal, Bonneton, P., Marieu, V., 2010. Two- and three-dimensional double-sandbar system behaviour under intense wave forcing and a meso-macro tidal range. Continental Shelf Research, 30 (7), 781-792.

Baldock, T.E., and D.A. Huntley (2002). Long wave forcing by the breaking of random gravity waves on a beach. Proc. R. Soc. A., 462, 1853-1876, doi:10.1098/rspa.2005.1642.

Battjes, J.A., H.J. Bakkenes, T.T. Janssen, and A.R. van Dongeren (2004), Shoaling of subharmonic gravity waves, J. Geophys. Res., 109, C02009, doi: 10.1029/2003JC001863.

Bryan, K.R., and G. Coco (2010). Observations of nonlinear runup patterns on plane and rythmic beach morphology. Journal of Geophysical research, 115, C09017, doi:10.1029/2009JC005721.

Bryan, K.R., and A.J. Bowen (1998), Bar-trapped edge waves and longshore currents. Journal of Geophysical research, 103(C12), 27867-27884, doi :10.1029/98JC02098.

Bryan, K.R., P.A. Howd, and A.J. Bowen (1998) Field observations of bar-trapped edge waves. Journal of Geophysical research, 103(C1), 1285-1305, doi :10.1029/98JC02938.Butel, R., H. Dupuis, and P. Bonneton, 2002. Spatial variability of wave conditions on the French Aquitanian coast using in-situ data, *In* : *Proceedings 7th International Coastal Symposium (Templepatrick, Northern Ireland), Journal of Coastal. Research*, SI36, 96-108.

Castelle, B., P. Bonneton, H. Dupuis, and N. Sénéchal, 2007. Double bar beach dynamics on the high energy meso-macrotidal French Aquitanian Coast : A review. *Marine. Geology*., 245, 141-159.

Coco, G., Werner, B.T., Burnet, T., and Elgar, S. (2004) The role of tides in beach cusp formation, J. Geophys. Res., 109, CO4011, doi: 10.1029/2003JC002154.

Elfrink, B., and T., Baldock (2002), Hydrodynamics and sediment transport in the swash zone: a review and perspectives, Coast. Eng., 45, 149-167.

Gallagher, E., J.H.M. MacMahan, Ad Reniers, J. Brown, and Ed Thornton (2011). Grain size variability on a rip-channeled beach. *Marine Geology*, 287(1-4):11.

Guedes, R.M.C., K.R. Bryan, and G. Coco (2012). Observations of alongshore variability of swash motions on a

intermediate beach. Continental Shelf research, 48(1), 61-74.
Guedes, R.M.C., K.R. Bryan, G. Coco, ad R. A. Holman (2011). The effects of tides on swash statistics on an intermediate beach. *Journal of Geophysical Research*, 116, C04008, doi:10.1029/2010JC006660.
Guza, R.T., and E.B., Thornton (1982), Swash oscillations on a natural beach, J. Geophys. Res., 87, 483-491.
Hendersen, S.M., R.T. Guza, S. Elgar, T.H.C. Herbers, and A.J. Bowen (2006), Nonlinear generation and loss of infragravity wave energy, J. Geophys. Res., 111, C12007, doi: 10.129/2006JC003539.
Holland, K.T. (1995), Foreshore dynamics : swash motions and topographic interactions on natural beaches, Ph.D. thesis, Oreg. State Univ., Corvallis, Oreg.
Holland, K.T., and R.A. Holman (1999), wavenumber-frequency structure of infragravity swash motions, J. Geophys. Res., 104, 13479-13488.
Holman, R.A. (1986), Extreme value statistics for wave run-up on a natural beach, Coast. Eng., 9, 527-544.
Holman, R.A., and A.H. Sallenger (1985), setup and swash on a natural beach, J. Geophys. Res., 90,945-953.
Janssen, T.T., J.A. Battjes, and A.R. Van Dongeren (2003). Long waves induced by short-wave groups over a sloping bottom. Journal of Geophysical Research, 108(C8), 3252, doi.10.1029/2002JC001515.
Masselink, G., and A.D. Short, 1993. The effect of the tide range on beach morphodynamics: a conceptual model. *Journal of Coastal Research*, 9, 785– 800.
Masselink, G., and M.G., Hughes (1998), Field investigation of sediment transport in the swash zone, *Cont. Shelf Res*., 18, 1179-1199.
Parisot, J.P., Capo, S., Castelle, B., Bujan, S., Moreau, J., Gervais, M., Réjas, A., Hanquiez, V., Almar, R., Marieu, V., Gaunet, J., Gluard, L., George, I., Nahon, A., Dehouck, A., Certain, R., Barthe, P., Le Gall, F., Bernardi, P.J., Le Roy, R., Pedreros, R., Delattre, M., Brillet, J., Sénéchal, N. (2009). Evolution of a multi-barred sandy beaches in presence of very energetic events. J. of Coastal Res., SI 56, 1786-1790.
Puleo, J.A., R.A. Beach, R.A. Holman, and J.S. Allen (2000), Swash zone sediment suspension and transport and the importance of bore-generated turbulence, J. Geophys. Res., 105, 17021-17044.
Raubenheimer, B., and R.T. Guza (1996), Observations and predictions of run-up, J. Geophys. Res., 101, 25575-25587.
Raubenheimer, B., R.T. Guza, S., Elgar, and N. Kobayashi (1995), Swash on a gently sloping beach, J. Geophys. Res., 100, 8751-8760.
Ruessink, B.G. (1998). The temporal and spatial variability of infragravity energy in a barred nearshore zone. Continental Shelf Research, 18, 585-605.
Ruessink, B.G., M.G., Kleinhans, and P.G.L., Van den Beukel (1998), Observations of swash under hihly dissipative conditions, J. Geophys. Res., 103, 3111-3118.
Ruggiero, P., P.D., Komar, J.J., Marra, W.G. McDougal, and R.A. Beach (2001), Wave runup, extreme water levels and the erosion of properties backing beaches, J. Coastal Res., 17, 407-419.
Ruggiero, P., R.A., Holman, and R.A. Beach (2004), Wave run-up on a high-energy dissipative beach, J. Geophys. Res, 109, C06025, doi:10.1029/2003JC002160.
Senechal, N., G. Coco, K.R. Bryan, ad R.A. Holman (2011a). Wave runup during extreme storm conditions. *Journal of Geophysical Research*, 116, C07032, doi:10.1029/2010JC006819.
Senechal, N., S. Abadie, F. Ardhuin, E. Gallagher, J.H.M. MacMahan, G. Masselink, H. Michallet, Ad J.H.M. Reniers, B.G. Ruessink, P.E. Russell, D. Sous, I.L. Turner, P. Bonneton, S. Bujan, S. Capo, R. Certain, T. Garlan, R. Pedreros, The ECORS-Truc Vert'08 field beach experiment: Presentation of a three-dimensional morphologic system in a macro-tidal environment during consecutive extreme storm conditions. Ocean Dynamics.
Stockdon, H.F., R.A. Holman, P.A. Howd, and A.H., Sallenger Jr. (2006), Empirical parameterization of setup, swash and runup, Coast. Eng., 53, 573-588.
Thomson, J., S. Elgar, B. Raubenheimer, T.H.C. Herbers, and R.T. Guza (2006), Tidal modulation of infragravity waves via nonlinear energy losses in the surf zone, Geophys. Res. Lett., 33, L05601, doi: 10.1029/2005GL025514.
Van Dongeren, A. R., J. Van Noorloos, K. Steenhauer, J.A. Battjes, T.T. Janssen, and A. Reniers (2004), Shoaling and shoreline dissipation of subharmonic gravity waves, in Proceedings, ICCE, edited by J. McKee Smith, 1225-1237, World Sci. Hackensack, N.J.
Van Dongeren, A. R., J., Battjes, T.T. Janssen, J. Van Noorloos, K. Steenhauer, G. Steenbergen, and A. Reniers (2007), Shoaling and shoreline dissipation of low-frequency waves, J. Geophys. Res. 112, C02011, doi. 10.1029/2006JC003701.
Wright, L.D., A.D. Short, and M.O. Green, 1984. Morphodynamic variability of surf zones and beaches: A synthesis. *Marine Geology*, 56, 93-118.